Derivation of a Six Degrees-of-Freedom Ground-Vehicle Model for Automotive Applications

Berntorp, Karl

2013

Document Version:
Publisher's PDF, also known as Version of record

Link to publication

Citation for published version (APA):
Berntorp, K. (2013). *Derivation of a Six Degrees-of-Freedom Ground-Vehicle Model for Automotive Applications*. (Technical Reports TFRT-7627). Department of Automatic Control, Lund Institute of Technology, Lund University.

Total number of authors:
1

LUND UNIVERSITY

PO Box 117
221 00 Lund
+46 46-222 00 00

ISSN 0280-5316
ISRN LUTFD2/TFRT--7627--SE

Derivation of a Six Degrees-of-Freedom Ground-Vehicle Model for Automotive Applications

Karl Berntorp

Lund University
Department of Automatic Control
February 2013

Lund University
Department of Automatic Control
Box 118
SE-221 00 Lund Sweden

Document name
TECHNICAL REPORT

Date of issue
February 2013

Document Number
ISRN LUTFD2/TFRT--7627--SE

Author(s)
Karl Berntorp

Supervisor

Sponsoring organization

Title and subtitle
Derivation of a Six Degrees-of-Freedom Ground-Vehicle Model for Automotive Applications

Abstract

Keywords

Classification system and/ or index terms (if any)

Supplementary bibliographical information

ISSN and key title
0280-5316

ISBN

Language
English

Number of pages
1-19

Recipient's notes

Security classification

http://www.control.lth.se/publications/

Contents

1. Introduction

This report contains derivations of a rigid double-track ground vehicle model including roll and pitch dynamics, using a Newton-Euler modeling approach. Suspension is incorporated in the model. The suspension system is modeled as a rotational spring and damper system, where the spring and damper constants for each wheel have been lumped to two constants, one for each degree of freedom. The resulting chassis model is of fifth order. The derivation can be found in Section 6. In addition, a first-order approach to take load transfer into account is discussed, which gives an additional degree of freedom. A schematic of the vehicle is shown in Figure 1. Wheel dynamics is also modeled, and several tire models that may be used together with the vehicle model are shown, which in conjunction gives a dynamic model on differential-algebraic form.

More or less complicated variants of the model can be found in literature. There exists numerous books and papers in the area of vehicle dynamics treating different aspects of vehicle modeling; see [Pacejka, 2006], [Ellis, 1994], [Isermann, 2006], [Kiencke and Nielsen, 2005], [Rajamani, 2006], [Gäfvert, 2003], [Schofield, 2008] for a few of them. However, they are often derived for a specific purpose, resulting in approximations appropriate for the problem considered. Moreover, important aspects of the derivations are often omitted in literature, resulting in a loss of insight. Also, it is hard to find a reference treating, in a compact way, the aspects of vehicle modeling considered in this report. Here, the model is derived with the aim of accurate simulation in general. The chassis model should also be possible to utilize for designing nonlinear controllers. If, for example, anti-rollover control is aimed for, it is reasonable to neglect pitch dynamics. The resulting model is presented in Section 7.

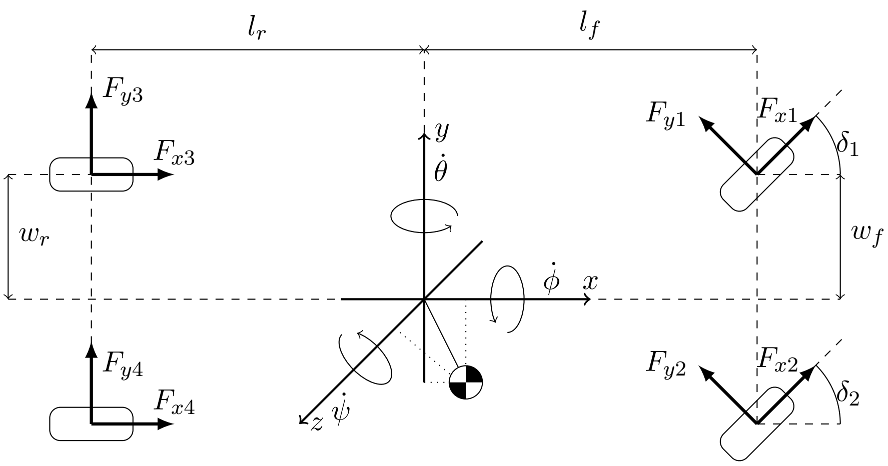

Figure 1 The vehicle model, with pitch dynamics as well as roll dynamics. The x and y-axes are residing in the ground plane. The wheels are numbered from the front left wheel to the rear right wheel.

2. Preliminaries

Vectors are denoted with a bar; that is, $\bar{v} = (v_x \quad v_y \quad v_z)^{\mathrm{T}}$ is a vector of dimension 3×1. Time derivatives of a vector with respect to a specific frame i are indicated with a subscript on the differential operator, as in $\frac{\mathrm{d}}{\mathrm{d}t}\big|_i \, \bar{v}$. Matrices are denoted with capital letters as in $\mathbf{A}$. Coordinate systems are denoted with S_i, where i is the letter indicating the frame.

3. Coordinate Systems

Three moving coordinate systems will be employed in the derivations, see Figure 2. The equations will be derived in the vehicle-fixed frame S_V, which is rotated with an angle ψ, the yaw, about the z-axis of the inertial frame S_E, yielding the rotation matrix

$$\mathbf{R}_V = \begin{pmatrix} \cos(\psi) & -\sin(\psi) & 0 \\ \sin(\psi) & \cos(\psi) & 0 \\ 0 & 0 & 1 \end{pmatrix}.$$

Moreover, the pitch θ is defined as a rotation about the y-axis of S_V, giving the chassis system S_C, with the rotation matrix

$$\mathbf{R}_C = \begin{pmatrix} \cos(\theta) & 0 & \sin(\theta) \\ 0 & 1 & 0 \\ -\sin(\theta) & 0 & \cos(\theta) \end{pmatrix}. \tag{1}$$

Finally, the body system S_B is defined by a rotation of an angle ϕ, the roll, about the x-axis of S_C:

$$\mathbf{R}_B = \begin{pmatrix} 1 & 0 & 0 \\ 0 & \cos(\phi) & -\sin(\phi) \\ 0 & \sin(\phi) & \cos(\phi) \end{pmatrix}. \tag{2}$$

The position of center of mass in the body frame is $\bar{h}_B = (0 \quad 0 \quad h)^{\mathrm{T}}$. With zero pitch and roll angle, this corresponds to the height over ground. Thus, the position of center of mass in the vehicle frame is given by $\bar{h}_V = \mathbf{R}_C\mathbf{R}_B\bar{h}_B$.

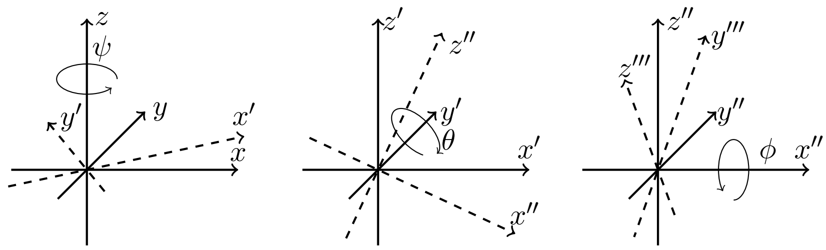

Figure 2 The coordinate systems used in the derivations. Note that the rotations are made with respect to the moving axes.

4. Kinematics

Denote with S_E an inertial frame. Further, denote with S_V a noninertial frame, rotating with the angular velocity vector $\bar{\omega}$ with respect to the inertial frame. Then, given a vector $\bar{v}$,

$$\left.\frac{\mathrm{d}}{\mathrm{d}t}\right|_E \bar{v} = \left.\frac{\mathrm{d}}{\mathrm{d}t}\right|_V \bar{v} + \bar{\omega} \times \bar{v}. \tag{3}$$

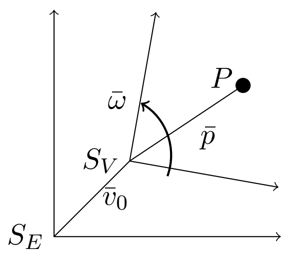

Figure 3 The inertial coordinate system, S_E, and the noninertial system, here denoted S_V. The noninertial frame is translating with velocity $\bar{v}_0$ and rotating with velocity $\bar{\omega}$.

Consider a point P with coordinates $\bar{p}$ with respect to S_V. The frame S_V is moving with translational velocity $\bar{v}_0$ with respect to S_E. Then the velocity of P is

$$\bar{v}_P = \bar{v}_0 + \left.\frac{\mathrm{d}}{\mathrm{d}t}\right|_E \bar{p} = \bar{v}_0 + \left.\frac{\mathrm{d}}{\mathrm{d}t}\right|_V \bar{p} + \bar{\omega} \times \bar{p}. \tag{4}$$

See Figure 3 for an illustration. By applying (3) to (4), the acceleration is found to be

$$\begin{aligned}\bar{a}_p &= \left.\frac{\mathrm{d}}{\mathrm{d}t}\right|_V \left(\bar{v}_0 + \left.\frac{\mathrm{d}}{\mathrm{d}t}\right|_V \bar{p} + \bar{\omega} \times \bar{p}\right) + \bar{\omega} \times \left(\bar{v}_0 + \left.\frac{\mathrm{d}}{\mathrm{d}t}\right|_V \bar{p} + \bar{\omega} \times \bar{p}\right) \\ &= \left.\frac{\mathrm{d}}{\mathrm{d}t}\right|_V \bar{v}_0 + \left.\frac{\mathrm{d}^2}{\mathrm{d}t^2}\right|_V \bar{p} + \left.\frac{\mathrm{d}}{\mathrm{d}t}\right|_V \bar{\omega} \times \bar{p} + \bar{\omega} \times \bar{v}_0 + \bar{\omega} \times (\bar{\omega} \times \bar{p}) + 2\bar{\omega} \times \left.\frac{\mathrm{d}}{\mathrm{d}t}\right|_V \bar{p}.\end{aligned} \tag{5}$$

In the subsequent sections, the time derivative of a quantity x will be denoted $\dot{x}$.

5. Kinetics

In a Newton-Euler setting, the total external forces acting on a rigid body $\mathcal{B}$ is defined by the identity

$$\int_{\mathcal{B}} \bar{a}_P \,\mathrm{d}m_P = m\bar{a}_G = \bar{F}, \tag{6}$$

where the integration is performed over all mass elements $\mathrm{d}m_P$. Further, $\bar{a}_G$ denotes the acceleration of center of mass. Likewise, the total external moments acting on the body equals

$$\left.\frac{\mathrm{d}}{\mathrm{d}t}\right|_E \int_{\mathcal{B}} \bar{p} \times \bar{v}_P \,\mathrm{d}m_P = \left.\frac{\mathrm{d}}{\mathrm{d}t}\right|_E \mathbf{I}_V \bar{\omega}_E = \bar{M}, \tag{7}$$

where $\bar{\omega}_E = (\dot{\phi} \quad \dot{\theta} \quad \dot{\psi})^{\mathrm{T}}$, and $\mathbf{I}_V$ is the moment of inertia matrix of the vehicle with respect to the vehicle-fixed frame. By applying (3) on (7) we get

$$\mathbf{I}_V \dot{\bar{\omega}}_E + \bar{\omega}_V \times \mathbf{I}_V \bar{\omega}_E = \bar{M}, \tag{8}$$

where $\bar{\omega}_V = (0 \quad 0 \quad \dot{\psi})^{\mathrm{T}}$ is the angular velocity of the frame in which the formulas are to be derived, in this case S_V. In (8), we have used that $\mathbf{I}_V$ is constant with respect to S_V. The moment of inertia is typically measured in the body frame, S_B. However, $\mathbf{I}_V$ can be found by using the formula $\mathbf{I}_V = \mathbf{R}_C \mathbf{R}_B \mathbf{I}_B \mathbf{R}_B^{\mathrm{T}} \mathbf{R}_C^{\mathrm{T}}$, where $\mathbf{I}_B$ is the moment of inertia in the body frame, and $\mathbf{R}_C$ and $\mathbf{R}_B$ are given by (1) and (2). For simplicity we have assumed that

$$\mathbf{I}_B = \begin{pmatrix} I_{xx} & 0 & 0 \\ 0 & I_{yy} & 0 \\ 0 & 0 & I_{zz} \end{pmatrix},$$

that is, cross terms are neglected. This gives that

$$\mathbf{I}_V = \begin{pmatrix} I_1 & I_2 & I_3 \\ I_2 & I_4 & I_5 \\ I_3 & I_5 & I_6 \end{pmatrix}, \tag{9}$$

where

$$\begin{aligned}
I_1 &= \cos^2(\theta) I_{xx} + \sin^2(\theta)\sin^2(\phi) I_{yy} + \sin^2(\theta)\cos^2(\phi) I_{zz}, \\
I_2 &= \sin(\theta)\sin(\phi)\cos(\phi)(I_{yy} - I_{zz}), \\
I_3 &= -\sin(\theta)\cos(\theta)\Big(I_{xx} - I_{yy} + \cos^2(\phi)(I_{yy} - I_{zz})\Big), \\
I_4 &= \cos^2(\phi) I_{yy} + \sin^2(\phi) I_{zz}, \\
I_5 &= \sin(\phi)\cos(\phi)\cos(\theta)(I_{yy} - I_{zz}), \\
I_6 &= \sin^2(\theta) I_{xx} + \cos^2(\theta)\Big(\sin^2(\phi) I_{yy} + \cos^2(\phi) I_{zz}\Big).
\end{aligned}$$

6. Vehicle Modeling

The total forces acting on the vehicle are found from force equilibriums in the x and y-directions, see Figure 1:

$$F_X = F_{x1}\cos(\delta_1) - F_{y1}\sin(\delta_1) + F_{x2}\cos(\delta_2) - F_{y2}\sin(\delta_2) + F_{x3} + F_{x4} \tag{10}$$
$$F_Y = F_{x1}\sin(\delta_1) + F_{y1}\cos(\delta_1) + F_{x2}\sin(\delta_2) + F_{y2}\cos(\delta_2) + F_{x3} + F_{x4} \tag{11}$$

By performing a torque equilibrium around the vehicle z-axis we find that

$$\begin{aligned}
M_Z = l_f\Big(&F_{x1}\sin(\delta_1) + F_{x2}\sin(\delta_2) + F_{y1}\cos(\delta_1) + F_{y2}\cos(\delta_2)\Big) \\
&+ w_f\Big(-F_{x1}\cos(\delta_1) + F_{x2}\cos(\delta_2) + F_{y1}\sin(\delta_1) - F_{y2}\sin(\delta_2)\Big) \\
&- l_r(F_{y3} + F_{y4}) - w_r(F_{x3} + F_{x4}).
\end{aligned} \tag{12}$$

To derive the model we first assume that the noninertial frame S_V is translating with velocity vector $\bar{v}$ relative to the inertial frame. By attaching S_V at the center of mass coordinates in the xy-plane, we get that $\bar{p} = 0$ in (4). Thus, the velocity in the x and y-directions are $\bar{v} = (v_x \quad v_y)^{\mathrm{T}}$.

The translational force equations can be found by combining (5), (6), (10), and (11). Note that we have assumed that $\bar{p}$ and all its derivatives are zero with respect to S_V. By reshuffling the equations we get:

$$\dot{v}_x = v_y\dot{\psi} + h\Big(\sin(\theta)\cos(\phi)(\dot{\psi}^2 + \dot{\phi}^2 + \dot{\theta}^2) - \sin(\phi)\ddot{\psi} - 2\cos(\phi)\dot{\phi}\dot{\psi}$$
$$- \cos(\theta)\cos(\phi)\ddot{\theta} + 2\cos(\theta)\sin(\phi)\dot{\theta}\dot{\phi} + \sin(\theta)\sin(\phi)\ddot{\phi}\Big) + \frac{F_X}{m} \quad (13)$$
$$\dot{v}_y = -v_x\dot{\psi} + h\Big(- \sin(\theta)\cos(\phi)\ddot{\psi} - \sin(\phi)\dot{\psi}^2 - 2\cos(\theta)\cos(\phi)\dot{\theta}\dot{\psi}$$
$$+ \sin(\theta)\sin(\phi)\dot{\phi}\dot{\psi} - \sin(\phi)\dot{\phi}^2 + \cos(\phi)\ddot{\phi}\Big) + \frac{F_Y}{m}. \quad (14)$$

The motion equation in the ψ-direction (about the z-axis) can be found by combining (8), (9), (10), (11), and (12). Note that because of the deflection of center of mass, the external forces in the x and y-directions give rise to additional external torques τ_z, in this case $\tau_z = -h(F_X \sin(\phi) + F_Y \sin(\theta)\cos(\phi))$:

$$\ddot{\psi}(I_{xx}\sin(\theta)^2 + \cos(\theta)^2(I_{yy}\sin(\phi)^2 + I_{zz}\cos(\phi)^2)) = M_Z - h\Big(F_X \sin(\phi)$$
$$+ F_Y \sin(\theta)\cos(\phi)\Big). \quad (15)$$

In the same manner we get the equation in the θ-direction as:

$$\ddot{\theta}(I_{yy}\cos(\phi)^2 + I_{zz}\sin(\phi)^2) = -K_\theta\theta - D_\theta\dot{\theta}$$
$$+ h\Big(mg\sin(\theta)\cos(\phi) - F_X\cos(\theta)\cos(\phi)\Big) + \dot{\psi}\Big(\dot{\psi}\sin(\theta)\cos(\theta)\big(\Delta I_{xy}$$
$$+ \cos(\phi)^2\Delta I_{yz}\big) - \dot{\phi}\cos(\theta)^2 I_{xx} + \sin(\phi)^2\sin(\theta)^2 I_{yy}$$
$$+ \sin(\theta)^2\cos(\phi)^2 I_{zz}) - \dot{\theta}\big(\sin(\theta)\sin(\phi)\cos(\phi)\Delta I_{yz}\big)\Big), \quad (16)$$

where K_θ and D_θ are the rotational spring and damping constants in the θ-direction. Further, $\Delta I_{yz} = I_{yy} - I_{zz}$ and $\Delta I_{xy} = I_{xx} - I_{yy}$. The third equation of angular motion is in the same manner found to be

$$\ddot{\phi}(I_{xx}\cos(\theta)^2 + I_{yy}\sin(\theta)^2\sin(\phi)^2 + I_{zz}\sin(\theta)^2\cos(\phi)^2) = -K_\phi\phi$$
$$- D_\phi\dot{\phi} + h(F_Y\cos(\phi)\cos(\theta) + mg\sin(\phi))$$
$$+ \dot{\psi}\Delta I_{yz}\Big(\dot{\psi}\sin(\phi)\cos(\phi)\cos(\theta) + \dot{\phi}\sin(\theta)\sin(\phi)\cos(\phi)\Big)$$
$$+ \dot{\psi}\dot{\theta}(\cos(\phi)^2 I_{yy} + \sin(\phi)^2 I_{zz}). \quad (17)$$

Equations (10)–(17) constitute the chassis double-track model with five degrees of freedom. With the addition of the load transfer Equations (34)–(39) in Section 9, the model is of sixth order.

7. Simplified Equations

For specific purposes different parts of the model can be neglected. For example, from a torque balance we can find an approximate condition for when rollover is imminent. Given this condition we can design a controller using the brakes as actuators. In this scenario we are primarily interested in the roll dynamics. Thus, we can neglect the pitch dynamics and the resulting equations become

$$
\begin{aligned}
m\dot{v}_x &= F_X + mv_y\dot{\psi} - mh\sin(\phi)\ddot{\psi} - 2mh\cos(\phi)\dot{\phi}\dot{\psi},\\
m\dot{v}_y &= F_Y - mv_x\dot{\psi} - mh\sin(\phi)\dot{\psi}^2 + mh\ddot{\phi}\cos(\phi) - m\dot{\phi}^2 h\sin(\phi),\\
\ddot{\psi} &= \frac{M_Z - F_X h\sin(\phi)}{I_{zz}\cos(\phi)^2 + I_{yy}\sin(\phi)^2},\\
I_{xx}\ddot{\phi} &= F_Y h\cos(\phi) + mgh\sin(\phi) + \dot{\psi}^2\Delta I_{yz}\sin(\phi)\cos(\phi) - K_\phi\phi - D_\phi\dot{\phi}.
\end{aligned}
$$

8. Ground-Tire Interaction

The vehicle model can be used directly by assuming that the longitudinal tire forces are control inputs. However, in a physical setup it is rather the wheel torques that are possible to control directly. By assuming direct controllability of the longitudinal tire forces, dynamics which in some situations is crucial is neglected.

The wheels are modeled as rotating masses with drive/brake torques and road contact tire forces, see Figure 4. When initiating the brake or drive pedal a torque is induced over the wheels, here referred to as M, which makes the wheels decelerate or accelerate.

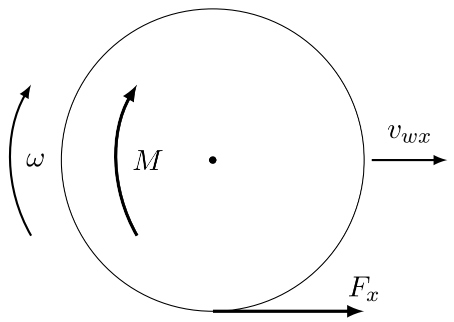

Figure 4 Wheel model.

From a torque balance around the center of the wheel, we find that

$$I_w\dot{\omega} = M - rF_x. \tag{18}$$

The notation is as follows:

- I_w is the moment of inertia of the wheel
- ω is the angular velocity of the wheel
- v_{wx} is the longitudinal velocity at the wheel
- r is the effective radius of the wheel
- F_x is the longitudinal force acting on the wheel.

When the driver brakes or accelerates, longitudinal slip develops. In [Schindler, 2007] this is defined as

$$\lambda = \frac{v_{wx} - r\omega}{v_{wx}} = 1 - \frac{r\omega}{v_{wx}} \tag{19}$$

when braking and

$$\lambda = \frac{v_{wx} - r\omega}{r\omega} = \frac{v_{wx}}{r\omega} - 1 \tag{20}$$

when accelerating. Here, v_{wx} is the component of the wheel velocity in the longitudinal direction, ω is the angular velocity of the wheel, and r is the effective wheel radius, that is the distance from the center of the wheel to the road. The normalization ensures that the slip is between -1 and 1.

The lateral slip angle is conventionally defined as

$$\tan\alpha = -\frac{v_{wy}}{v_{wx}}, \tag{21}$$

where v_{wx} and v_{wy} are the longitudinal and lateral wheel velocity, see Figure 5. The wheel velocities can be found by using trigonometry and the velocity of the center of mass, known from Section 6. A convenient approach is then to define lateral slip as $\sin\alpha$. The definition ensures that the slip is between -1 and 1. The third slip quantity

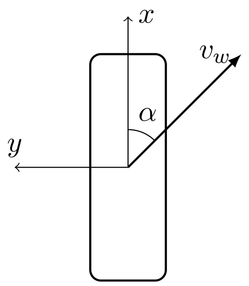

Figure 5 The wheel together with its coordinate system seen from above.

considered is the vehicle body sideslip angle β, which is defined through the vehicle's longitudinal and lateral velocity as

$$\tan\beta = \frac{v_y}{v_x}. \tag{22}$$

The nominal tire forces; that is, the forces under pure slip conditions which are to be used in (18), can be computed with the Magic Formula model [Pacejka, 2006], given by

$$F_0(m) = D\sin\Big(C\arctan\big(Bm - E(Bm - \arctan(Bm))\big)\Big), \tag{23}$$

where

- B is the stiffness factor
- C is the shape factor
- D is the peak factor
- E is the curvature factor
- F_0 is either the longitudinal or lateral force and m is either λ or α.

The typical shape of (23) for a high friction surface is Shown in Figure 6, where μ is the friction coefficient.

Another formula often used to model lateral forces is the *Highway Safety Research Institute (HSRI) Tire Model*[1], see Figure 7. The following formulas are taken from [Klěcka, 2007]:

$$F_y = \begin{cases} C_\alpha \cdot \frac{\tan\alpha}{1+\lambda} & \text{if } s_r \le 0.5 \\ C_\alpha \cdot \frac{\tan\alpha}{1+\lambda} \cdot \frac{s_r - 0.25}{s_r^2} & \text{if } s_r > 0.5 \end{cases} \tag{24}$$

where

$$s_r = \frac{\sqrt{(C_\lambda \lambda)^2 + (C_\alpha \tan\alpha)^2}}{\mu(1+\lambda)F_z}$$

and C_α and C_λ denote the initial slopes of the force curves. The HSRI equations do not exhibit any force peak, and may thus mimic the true force poorly for high-friction surfaces. Still, the model is sometimes used in traction control systems, see [Berntorp, 2008].

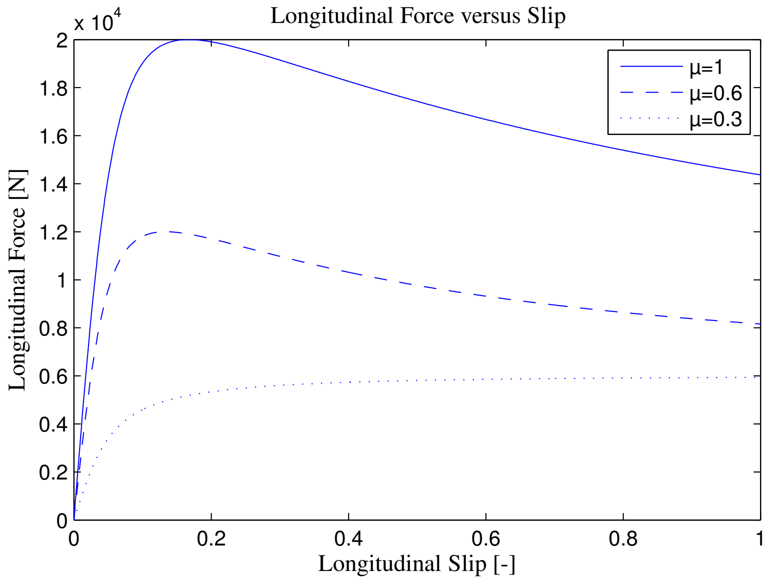

Figure 6 The tire-force model generated by the Magic formula (23) for different surfaces using a typical set of parameters. The friction between road and tire is denoted with μ.

8.1 Friction Ellipse

One way to model combined slip is to use the idea of the *friction ellipse*. The idea is that the longitudinal and lateral forces are described by

$$\left(\frac{F_x}{F_{x,\max}}\right)^2 + \left(\frac{F_y}{F_{y,\max}}\right)^2 = 1.$$

When using the brakes as actuators the longitudinal forces can be seen as control inputs, and then the above equation can be used to calculate F_y as

$$F_y = F_{y0}\sqrt{1 - \left(\frac{F_x}{\mu_x F_z}\right)^2}. \tag{25}$$

[1]Also known as the Dugoff Tire Model.

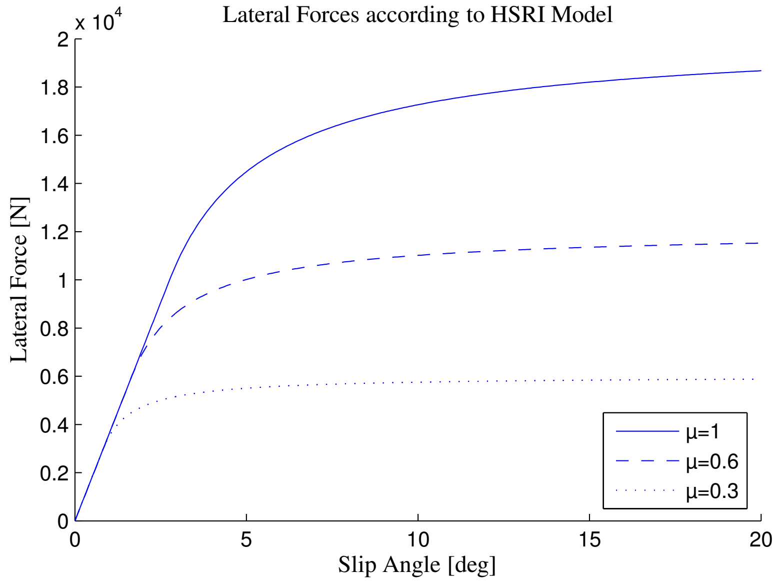

Figure 7 The HSRI tire model.

In (25), F_{y0} can be taken from a suitable tire model, for example the Magic formula or the HSRI model. However, it is also possible to use the longitudinal slip λ as an input. Then the force equations become [Isermann, 2006]

$$F_x = \frac{\lambda}{\sqrt{\lambda^2 + \alpha^2}} F_{\text{res}} \tag{26}$$

$$F_y = \frac{\alpha}{\sqrt{\lambda^2 + \alpha^2}} F_{\text{res}} \tag{27}$$

where F_{res} is the resulting force. Figure 8 shows how the lateral force changes with λ for some given values of α according to (27), which is a good approximation in many driving situations. The impact of α on the longitudinal force can also be illustrated by Figure 8.

8.2 Weighting Functions

Another approach to model combined slip is described in [Pacejka, 2006]. Here, the idea is to scale the nominal forces, (23), for each wheel with weighting functions, G_α and G_λ, depending on α and λ. The relations in the longitudinal (x) direction are

$$B_\alpha = B_{\alpha,1} \cos(\arctan(B_{\alpha,2}\lambda)), \tag{28}$$

$$G_\alpha = \cos(C_\alpha \arctan(B_\alpha \alpha)), \tag{29}$$

$$F_x = F_{x0} G_\alpha. \tag{30}$$

The corresponding relations in the y-direction are given by

$$B_\lambda = B_{\lambda,1} \cos(\arctan(B_{\lambda,2}(\alpha_i - B_{\lambda,i}))), \tag{31}$$

$$G_\lambda = \cos(C_\lambda \arctan(B_\lambda \lambda)), \tag{32}$$

$$F_y = F_{y0} G_\lambda. \tag{33}$$

This way of modeling combined slip has been experimentally verified [Braghin *et al.*, 2006]. The difference in shape compared to the friction ellipse can be seen in Figure 9. The main difference is that for the weighting functions the longitudinal force decreases when the lateral force approaches zero.

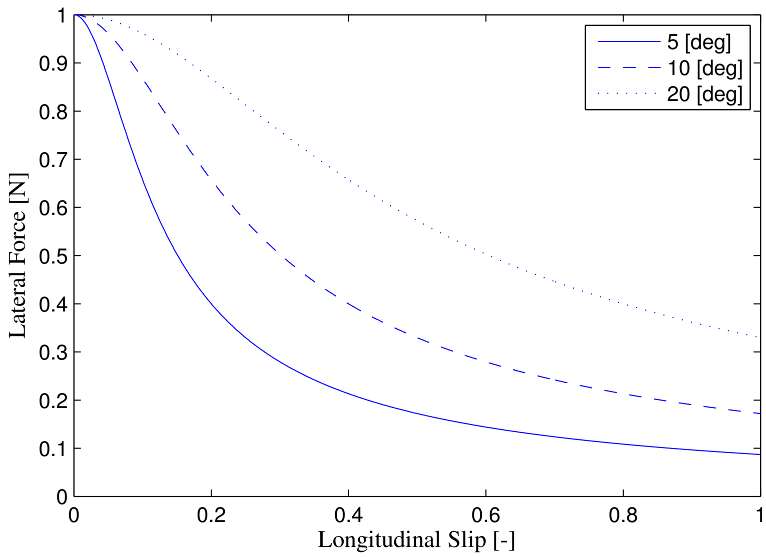

Figure 8 Longitudinal slip impact on the lateral force for some values of α taken from (27).

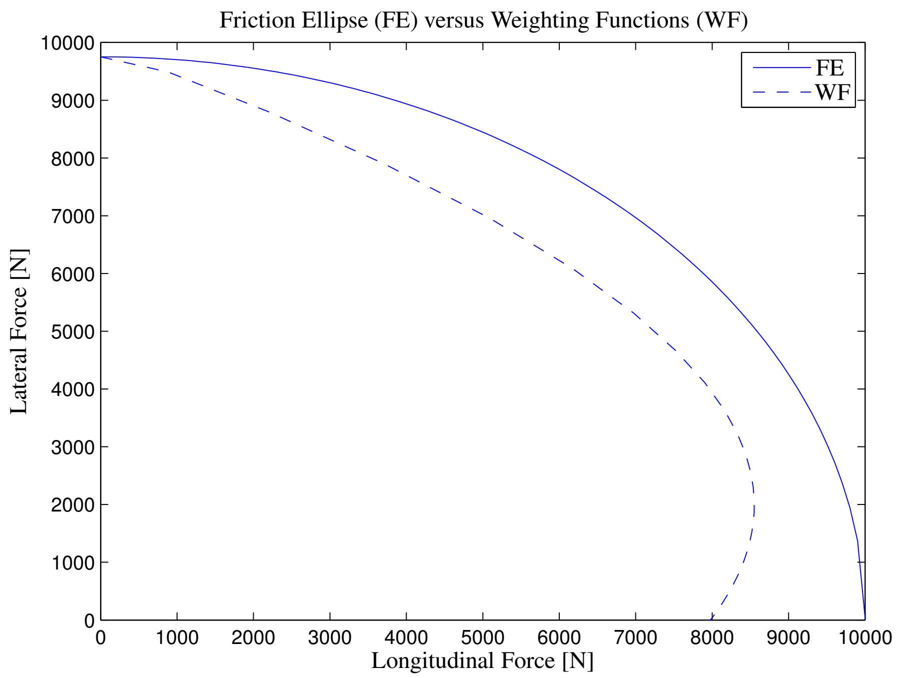

Figure 9 Combined tire forces for the friction ellipse (Equations (26)–(27)) and the weighting functions (Equations (28)–(33)). The slip angle is set to $\alpha = 14$ [deg].

9. Load Transfer

The pitch and roll dynamics do not only influence the yaw and translational dynamics, but also the load resting on each wheel. Further, the pitch and roll also affect the parameters in (23). To establish how the pitch and roll influence Equation (23) is a difficult problem, but to get a good approximation of the load transfer is rather easy. A first approach is to assume that the pitch and roll angles influence the load transfer independently, which should be a reasonable approximation for small angles. Then a torque equilibrium gives that the change in lateral force caused by the roll for each front and rear wheel, respectively, is

$$\Delta F_{z,1} = -\frac{K_\phi \phi + D_\phi \dot{\phi}}{4w_f}, \tag{34}$$

$$\Delta F_{z,2} = \frac{K_\phi \phi + D_\phi \dot{\phi}}{4w_f}, \tag{35}$$

$$\Delta F_{z,3} = -\frac{K_\phi \phi + D_\phi \dot{\phi}}{4w_r}, \tag{36}$$

$$\Delta F_{z,4} = \frac{K_\phi \phi + D_\phi \dot{\phi}}{4w_r}. \tag{37}$$

In the same way we find the load transfer for the front wheels caused by the pitch as

$$\Delta F_{z,f} = \frac{K_\theta \theta + D_\theta \dot{\theta}}{4l_f}, \tag{38}$$

and the load transfer for the rear wheels is

$$\Delta F_{z,r} = -\frac{K_\theta \theta + D_\theta \dot{\theta}}{4l_r}. \tag{39}$$

This load transfer model will fit the true load well for modest combined roll and pitch angles. However, if (very) high accuracy is needed, approaches which take into account coupling effects are necessary.

10. Conclusions

A six degrees-of-freedom ground-vehicle model was derived using a Newton-Euler approach. It is a general purpose model suitable both for high-accuracy simulation as well as for nonlinear control design. In addition, ground-tire interaction modeling using different force-tire models were discussed, both for pure and combined slip. Finally, a first approach to load transfer modeling was mentioned.

11. References

Berntorp, K. (2008): “ESP for suppression of jackknifing in an articulated bus.” Master’s Thesis ISRN LUTFD2/TFRT--5831--SE. Department of Automatic Control, Lund University, Sweden.

Braghin, F., F. Cheli, and E. Sabbioni (2006): “Environmental effects on Pacejka’s scaling factors.” *Vehicle System Dynamics: International Journal of Vehicle Mechanics and Mobility*, **44:7**, pp. 547–568.

Ellis, J. R. (1994): *Vehicle Handling Dynamics*. Mechanical Engineering Publications, London, United Kingdom.

Gäfvert, M. (2003): *Topics in Modeling, Control, and Implementation in Automotive Systems*. PhD thesis ISRN LUTFD2/TFRT--1066--SE, Department of Automatic Control, Lund University, Sweden.

Isermann, R. (2006): *Fahrdynamik-Regelung: Modellbildung, Fahrerassistenzsysteme, Mechatronik.* Vieweg-Verlag, Wiesbaden, Germany.

Kiencke, U. and L. Nielsen (2005): *Automotive Control Systems—For Engine, Driveline and Vehicle*, second edition. Springer-Verlag, Berlin Heidelberg.

Klěcka, R. (2007): “Vehicle Model for Dynamics Analysis and HIL Simulation.” Technical Report. Department of Control Systems and Instrumentation, Faculty of Mechanical Engineering, Technical University of Ostrava.

Pacejka, H. B. (2006): *Tyre and Vehicle Dynamics*, second edition. Butterworth-Heinemann, Oxford, United Kingdom.

Rajamani, R. (2006): *Vehicle Dynamics and Control.* Springer-Verlag, Berlin Heidelberg.

Schindler, E. (2007): *Fahrdynamik: Grundlagen Des Lenkverhaltens Und Ihre Anwendung Für Fahrzeugregelsysteme.* Expert-Verlag, Renningen, Germany.

Schofield, B. (2008): *Model-Based Vehicle Dynamics Control for Active Safety.* PhD thesis ISRN LUTFD2/TFRT--1083--SE, Department of Automatic Control, Lund University, Sweden.

Appendix

Symbol	Description
x	Longitudinal position
y	Lateral position
h	center of mass height in body frame
g	Gravitational constant
I_{xx}	Moment of inertia about center of mass x-axis
I_{yy}	Moment of inertia about center of mass y-axis
I_{zz}	Moment of inertia about center of mass z-axis
I_w	Wheel moment of inertia
ψ	Yaw angle
θ	Pitch angle
ϕ	Roll angle
δ	Steering angle (at the wheels)
α	Wheel tire slip angle
β	Sideslip angle
ω	Angular velocity
λ	Longitudinal slip
l_f	Distance between center of mass and front axle
l_r	Distance between center of mass and rear axle
w_f	Front half-track width
w_r	rear half-track width
r	Effective wheel radius
v_{wx}	Wheel longitudinal velocity
v_{wy}	Wheel lateral velocity
F_x	Longitudinal tire force
F_y	Lateral tire force
F_z	Vertical tire force
F_0	Force in Magic formula
M	Torque
B	Stiffness factor in Magic formula
C	Shape factor in Magic formula
D	Peak factor in Magic formula
E	Curvature factor in Magic formula